Slanted n-ZnO nanorod arrays/p-GaN light-emitting diodes with strong ultraviolet emissions

Zu-Po Yang,[1] Zhong-Han Xie,[2] Chia-Ching Lin,[1] and Ya-Ju Lee [2,*]

[1]*Institute of Photonic System, National Chiao Tung University, Tainan City 71150, Taiwan*
[2]*Institute of Electro-Optical Science and Technology, National Taiwan Normal University, 88, Sec.4, Ting-Chou Road, Taipei 116, Taiwan*
**yajulee@ntnu.edu.tw*

Abstract: Both of oblique angle deposition and conventional deposition techniques were used by a RF sputtering system to grow the slanted (β = 32°) and planar (β = 0°) n-ZnO films on p-GaN, respectively. These two kinds of n-ZnO/p-GaN heterojunctions were then fabricated the light-emitting diodes (LEDs). The electrical and optical properties of these two kinds of LEDs were investigated systematically. The results show that the slanted n-ZnO/p-GaN LEDs have a lower turn-on voltage and less leakage current than that of planar n-ZnO/p-GaN LEDs. Moreover, different from the planar n-ZnO/p-GaN LEDs which emitting colors changes with injection current, the slanted n-ZnO/p-GaN LEDs retains UV emissions (385-400 nm) under the entire range of injection currents we applied. The dominant UV luminescence of slanted n-ZnO/p-GaN LEDs is attributed to the ZnO near band edge transitions, indicating the high quality of slanted ZnO films and exhibiting the essential property dedicated to nano-sized heterojunctions. Hence, we have demonstrated that the slanted n-ZnO/p-GaN LEDs fabricated by oblique angle deposition have better performance than the planar n-ZnO/p-GaN LEDs fabricated by convention deposition means.

OCIS codes: (230.3670) Light-emitting diodes; (160.6000) Semiconductor materials; (220.4241) Nanostructure fabrication.

References and links

1. A. Tsukazaki, A. Ohtomo, T. Onuma, M. Ohtani, T. Makino, M. Sumiya, K. Ohtani, S. F. Chichibu, S. Fuke, Y. Segawa, H. Ohno, H. Koinuma, and M. Kawasaki, "Repeated temperature modulation epitaxy for p-type doping and light-emitting diode based on ZnO," Nat. Mater. **4**(1), 42–46 (2004).
2. D. M. Bagnall, Y. F. Chen, Z. Zhu, T. Yao, M. Y. Shen, and T. Goto, "High temperature excitonic stimulated emission from ZnO epitaxial layers," Appl. Phys. Lett. **73**(8), 1038–1040 (1998).
3. Z. L. Wang, "Zinc oxide nanostructures: growth, properties and applications," J. Phys. Condens. Matter **16**(25), R829–R858 (2004).
4. C. Y. Huang, Y. J. Lee, T. Y. Lin, S. L. Chang, J. T. Lian, H. M. Lin, N. C. Chen, and Y. J. Yang, "Direct formation of InN-codoped p-ZnO/n-GaN heterojunction diode by solgel spin-coating scheme," Opt. Lett. **39**(4), 805–808 (2014).
5. B. Xiang, P. W. Wang, X. Z. Zhang, S. A. Dayeh, D. P. R. Aplin, C. Soci, D. P. Yu, and D. L. Wang, "Rational Synthesis of p-Type Zinc Oxide Nanowire Arrays Using Simple Chemical Vapor Deposition," Nano Lett. **7**(2), 323–328 (2007).
6. Ya. I. Alivov, J. E. Van Nostrand, D. C. Look, M. V. Chukichev, and B. M. Ataev, "Observation of 430 nm electroluminescence from ZnO/GaN heterojunction light-emitting diodes," Appl. Phys. Lett. **83**(14), 2943–2945 (2003).
7. H. Huang, G. Fang, Y. Li, S. Li, X. Mo, H. Long, H. Wang, D. L. Carroll, and X. Zhao, "Improved and color tunable electroluminescence from n-ZnO/HfO2/p-GaN heterojunction light emitting diodes," Appl. Phys. Lett. **100**(23), 233502 (2012).
8. Y. Chen, D. Bagnall, and T. Yao, "ZnO as a novel photonic material for the UV region," Mater. Sci. Eng. B **75**(2–3), 190–198 (2003).
9. A. M. C. Ng, Y. Y. Xi, Y. F. Hsu, A. B. Djurišić, W. K. Chan, S. Gwo, H. L. Tam, K. W. Cheah, P. W. K. Fong, H. F. Lui, and C. Surya, "GaN/ZnO nanorod light emitting diodes with different emission spectra," Nanotechnology **20**(44), 445201 (2009).

#229127 - $15.00 USD Received 8 Dec 2014; revised 7 Jan 2015; accepted 14 Jan 2015; published 21 Jan 2015

10. H. C. Chen, M. J. Chen, M. K. Wu, W. C. Li, H. L. Tsai, J. R. Yang, H. Kuan, and M. Shiojiri, "UV Electroluminescence and Structure of n-ZnO/p-GaN Heterojunction LEDs Grown by Atomic Layer Deposition," IEEE J. Quantum Electron. **46**(2), 265–271 (2010).
11. P. F. Carcia, R. S. McLean, M. H. Reilly, and G. Nunes, "Transparent ZnO thin-film transistor fabricated by rf magnetron sputtering," Appl. Phys. Lett. **82**(7), 1117–1119 (2003).
12. J. Q. Xi, M. F. Schubert, J. K. Kim, E. F. Schubert, M. Chen, S. Y. Lin, W. Liu, and J. A. Smart, "Optical thin-film materials with low refractive index for broadband elimination of Fresnel reflection," Nat. Photonics **1**, 176–179 (2007).
13. R. Teki, T. C. Parker, H. Li, N. Korotkar, T. M. Lu, and S. Lee, "Low temperature synthesis of single crystalline ZnO nanorods by oblique angle deposition," Thin Solid Films **516**(15), 4993–4996 (2008).
14. J. M. LaForge, M. T. Taschuk, and M. J. Brett, "Glancing angle deposition of crystalline zinc oxide nanorods," Thin Solid Films **519**(11), 3530–3537 (2011).
15. C. Y. Chen, J. H. Huang, K. Y. Lai, Y. J. Jen, C. P. Liu, and J. H. He, "Giant optical anisotropy of oblique-aligned ZnO nanowire arrays," Opt. Express **20**(3), 2015–2024 (2012).
16. D. Toledano, R. E. Galindo, M. Yuste, J. M. Albella, and O. Sanchez, "Compositional and structural properties of nanostructured ZnO thin films grown by oblique angle reactive sputtering deposition: effect on the refractive index," J. Phys. D Appl. Phys. **46**(4), 045306 (2013).
17. Y. J. Lee, Z. P. Yang, J. J. Siao, Z. H. Xie, Y. L. Chuang, T. Y. Lin, and J. K. Sheu, "Slanted n-ZnO/p-GaN nanorod arrays light-emitting diodes grown by oblique-angle deposition," APL Material **2**(5), 056101 (2014).
18. Y.-C. Yao, M.-T. Tsai, H.-C. Hsu, L.-W. She, C.-M. Cheng, Y.-C. Chen, C.-J. Wu, and Y.-J. Lee, "Use of two-dimensional nanorod arrays with slanted ITO film to enhance optical absorption for photovoltaic applications," Opt. Express **20**(4), 3479–3489 (2012).
19. Y.-J. Lee, Y.-C. Yao, and C.-H. Yang, "Direct electrical contact of slanted ITO film on axial p-n junction silicon nanowire solar cells," Opt. Express **21**(S1 Suppl 1), A7–A14 (2013).
20. V. Tvarrozek, I. Novotny, P. Sutta, M. Netrvalova, I. Vavra, J. Bruncko, P. Gaspierik, and S. Flickyngerova, "Oblique Angle Sputtering of ZnO:Ga Thin Films," Physics Procedia **32**, 456–463 (2012).
21. J. K. Sheu, K. W. Shu, M. L. Lee, C. J. Tun, and G. C. Chi, "Effect of Thermal Annealing on Ga-Doped ZnO Films Prepared by Magnetron Sputtering," J. Electrochem. Soc. **154**(6), H521–H524 (2007).
22. A. Janotti and C. G. V. Walle, "Native point defects in ZnO," Phys. Rev. B **76**(16), 165202 (2007).
23. K. Ellmer, "Resistivity of polycrystalline zinc oxide films: current status and physical limit," J. Phys. D Appl. Phys. **34**(21), 3097–3108 (2001).
24. S. Xu, C. Xu, Y. Liu, Y. Hu, R. Yang, Q. Yang, J. H. Ryou, H. J. Kim, Z. Lochner, S. Choi, R. Dupuis, and Z. L. Wang, "Ordered Nanowire Array Blue/Near-Uv Light Emitting Diodes," Adv. Mater. **22**(42), 4749–4753 (2010).
25. R. A. Rosenberg, M. Abu Haija, K. Vijayalakshmi, J. Zhou, S. Xu, and Z. L. Wang, "Depth resolved luminescence from oriented ZnO nanowires," Appl. Phys. Lett. **95**(24), 243101 (2009).
26. X. Y. Xu, Y. C. Liu, Y. X. Liu, C. S. Xu, C. L. Shao, and R. Mu, "Ultraviolet electroluminescence from p-GaN/i-ZnO/n-ZnO heterojunction light-emitting diodes," Appl. Phys. B **80**(7), 871–874 (2005).

1. Introduction

Zinc oxide (ZnO) has attracted great attention recently for the applications of blue/near UV optoelectronic devices, e.g. light-emitting diodes (LEDs) [1], due to its unique properties such as direct wide bandgap energy of 3.37 eV, large exciton binding energy of 60 meV, and high radiation hardness for harsh environment operation [2, 3]. However, the fabrication of homojunction ZnO LEDs is hindered by its intrinsic n-type polarity [4] and difficulty to achieve reproducible and stable p-type ZnO material [5]. Therefore, alternative approach of using ZnO heterojunction structures, which are composed of n-type ZnO and other p-type materials, has been proposed [6, 7]. Among them, p-GaN is one of the best candidates in consideration of same wurtzite structure and small lattice mismatch of ~1.9%. Since the GaN LEDs have been well developed in industry, n-ZnO/p-GaN heterojunction structures are typically prepared by deposited n-ZnO film on top of p-GaN using various deposition techniques, such as molecular beam epitaxy [8], metal-organic chemical vapor deposition (MOCVD) [9], pulsed laser deposition (PLD) [1], atomic layer deposition (ALD) [10], and radio-frequency (RF) magnetron sputtering [11]. Among them, sputtering is one of the popular techniques for providing high-quality and cost-effective ZnO films. Different from techniques of conventional physical deposition with vapor flux normal to the substrate, oblique angle deposition (OAD) technique controls the incident angle of incoming vapor flux to produce nanostructure thin films. Due to the geometric shadowing effect, OAD has successfully produced slanted-nanorod/column oxide layers (TiO_2 and SiO_2 nanorod arrays) [12] rather than planar films produced by conventional physical deposition, and that was mainly applied on the photovoltaics because the produced nanoporous film can virtually

#229127 - $15.00 USD Received 8 Dec 2014; revised 7 Jan 2015; accepted 14 Jan 2015; published 21 Jan 2015

eliminate the Fresnel reflection over a broadband of solar spectrum by precise control of its refractive index through tuning the incident angle of vapour flux. Recently, there are many research works about using OAD to grow ZnO nanostructure thin films [13–16]. However, most of works focus on the crystalline point of view such as morphology and crystal orientation [13, 14]. For the optical properties of OAD ZnO films, their birefringence due to anisotropic nanostructure has been investigated [15, 16]. To date, there are only few works of using OAD to fabricate ZnO LEDs [17], especially for ZnO/GaN heterojunction LEDs. In [17], the slanted n-ZnO/p-GaN nanorod array LEDs were fabricated by the dry etching (to fabricate p-GaN nanorods) and OAD of ZnO in sequence. However, since OAD can produce nano-rods/columns directly, this motivates us to fabricate the slanted ZnO nanorods on p-GaN without the need of dry etching step, which can save the cost of nanorod LEDs fabrication. However, the feasibility of this ideal depends strongly on the quality and performance of ZnO film produced by OAD and how its quality and performance compare with the ZnO film produced by conventional method. In addition, the comparison of ZnO film produced by conventional method with that produced by OAD is also important and might affect the feasibility of our previous proposal [17]. This has not been investigated systematically in our previous work, because we cannot produce ZnO nanorods on GaN nanorod using conventional deposition method due to no geometric shadowing effect.

In this work, we used conventional deposition and OAD by RF sputtering to grow the planar and slanted n-ZnO films, respectively, on top of p-GaN, which form the nano-sized n-ZnO/p-GaN heterojunctions for the fabrication of LEDs. The optical and electrical properties of these two kinds of LEDs have been investigated systematically. In comparison, the slanted n-ZnO/p-GaN LEDs not only show a lower turn-on voltage and less leakage current, but also emit strong and stable UV luminescence in the regime of 385-400 nm as we increase the injection current. Hence, we have demonstrated that the slanted n-ZnO/p-GaN LEDs have better performance than the planar n-ZnO/p-GaN LEDs, and offer a great potential for the next generation of high-efficient LED structure.

2. Experiments

Figure 1(a) shows the schematic of slanted (β = 32°) n-ZnO/p-GaN LEDs. The conventional n-ZnO/p-GaN LEDs have similar design but replace slanted ZnO film with the planar (β = 0°) ZnO film. Entire ZnO/GaN heterostructures are composed of 2-μm-thick undoped GaN buffer layer on top of (0001) sapphire substrate, followed by a 400-nm-thick p-GaN with hole concentration of $p = 5.5 \times 10^{17}$ cm^{-3} and mobility of $\mu_p = 6.2$ $cm^2/V\text{-}s$. Both of GaN layers were grown by MOCVD. Then the planar and slanted ZnO films of 300 nm were grown on top of p-GaN by conventional deposition and OAD, respectively, using a RF sputtering system at room temperature. In the ZnO deposition, the 99%-pure ZnO sputtering target with diameter of 76.4 mm is separated from the substrate by a distance of 70 mm. The incident angle of ZnO vapor flux to substrate is controlled by the tilting angle of sample holder. For the planar and slanted ZnO films, the tilting angle is set at 0 and 60 degree, respectively. Before the deposition, the chamber was first pumped down to 5×10^{-6} torr, then oxygen (99.99%) and argon gases (99.999%) in the flow ratio of 2 sccm to 20 sccm were introduced into the chamber. During the ZnO deposition, the chamber pressure and RF power were maintained at 8×10^{-3} torr and 100 W, respectively. The top view of scanning electron microscopy (SEM) image of slanted ZnO film is shown in the Fig. 1(b). The surface morphology of the slanted ZnO films shows the dome-like feature with different sizes, which might relate to the top surfaces of slanted rods/columns. In order to optimize the annealing temperature for the deposited ZnO films and examine the quality of ZnO films after annealing, another two sets of planar and slanted ZnO films were also grown on sapphire substrate directly in the same deposition conditions. Figures 1(c) and 1(d) show cross-sectional SEM images of the planar and slanted ZnO films on sapphire, respectively. This confirms that OAD can produce slanted ZnO rods/columns with titling angle β of 32° respect to the surface normal. Both of the deposited planar and slanted ZnO films on sapphire were

#229127 - $15.00 USD Received 8 Dec 2014; revised 7 Jan 2015; accepted 14 Jan 2015; published 21 Jan 2015

then annealed at 600–1000 °C with a 100 °C interval for 1min. under a nitrogen atmosphere. These films were analyzed by θ-2θ scan of X-ray diffraction (XRD). The possible stacking way of wurtize lattice for slanted ZnO nano-column/rod is schematically drew and also inserted in Fig. 1(d). Further studies are needed to understand the detail and exact stacking mechanisms and configurations of wurtize lattice for our slanted ZnO nano-column/rod. The LEDs with chip size of 300 μm × 400 μm were then fabricated by regular photolithography and deposition of Ni (10nm) and ITO (250nm) in sequence for the electrical contacts. After 2-minute rapid thermal process at temperature of 450 °C in nitrogen ambient (500 torr), the linear current-voltage characteristics can be obtained. The specific contact resistances of ITO/Ni/p-GaN and ITO/Ni/n-ZnO are 5.02×10^{-4} and 9.66×10^{-4} Ω-cm^2, respectively, which is acceptable in terms of the metallization scheme of LEDs. It shall be addressed that to make a fair comparison of device's performances between planar and slanted ZnO/p-GaN LEDs, the fabricated processes of both samples are identical except the shape of ZnO films.

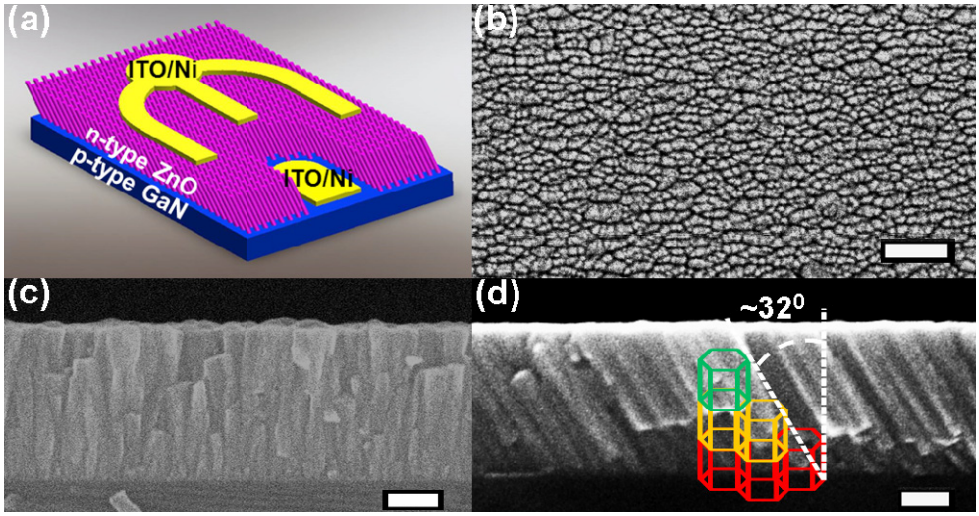

Fig. 1. (a) The schematic of the slanted n-ZnO/p-GaN LEDs. (b) The top-view SEM image of the slanted ZnO film. The cross-sectional SEM images of (c) planar and (d) slanted ZnO films. The slanted ZnO rods/columns exhibit titling angle of 32° respect to surface normal. The possible stacking way of wurtize lattice for slanted ZnO film is also shown. The scale bar is 100 nm.

To characterize the crystallinity, electrical, and optical properties of the samples, X-ray diffraction (XRD), Hall measurement, current-voltage (I-V) curve, photoluminescence (PL) measurement, and electroluminescence (EL) measurement were conducted. The crystallinity of sample was analyzed by θ-2θ scan of XRD using Kα line with wavelength of 1.54Å. The electrical carrier concentration and mobility were extracted by a Hall measurement system using van der Pauw method. The current versus voltage (I-V) curve was measured by a Keithley 2400 SourceMeter at room temperature in dark environment to minimize the effect of ambient light. For the PL measurement, a HeCd laser (λ = 325nm) was used the optical pumping source, and the laser's output power and beam size on the sample is 1.6mW and 1.0mm, respectively. By assuming all the pumping photons can excite electrons to conduction band without any loss, the pumping carrier density is estimated to be ~2.75×10^{17}/cm^2-sec. The emission lights from samples were collected and then sent into a monochromator equipped with a photomultiplier (PMT) detector. For the EL measurement, the setup is similar to the PL measurement but replaces the optical pumping source with an electrical bias.

#229127 - $15.00 USD Received 8 Dec 2014; revised 7 Jan 2015; accepted 14 Jan 2015; published 21 Jan 2015

3. Results and discussions

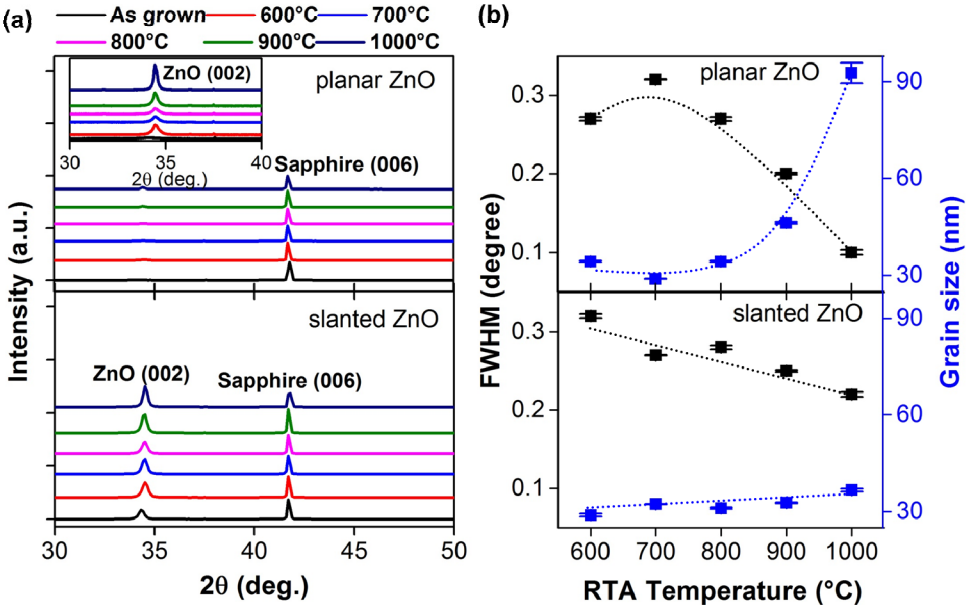

Fig. 2. (a) The XRD curves for the as-grown and post-annealed samples of planar (top) and slanted (bottom) ZnO films on sapphire. The inset of top panel shows the zoom in of planar ZnO (002) peak. (b) The FWHM of (002) peak and average grain size of planar (top) and slanted (bottom) ZnO films versus RTA temperature. The dashed lines are the guides to eye.

Figure 2(a) shows the θ-2θ scan of XRD for the as-grown and post-annealed samples of planar (top) and slanted (bottom) ZnO films on sapphire. Two diffraction peaks around $2\theta = 34.5°$ and $2\theta = 41.68°$ are observed, corresponding to the (002) plane of ZnO and (006) plane of sapphire, respectively. The observation of (002) peak of ZnO indicates that the films grow along the c-axis of wurtzite structure and retain c-axis orientation after anneal. The intensity of all slanted ZnO (002) peaks is comparable with the intensity of sapphire (006) peak; however, the intensity of all planar ZnO (002) peak is much weaker than that of sapphire (006) peak. The zoom in of planar ZnO (002) peak is shown in the inset of the top panel of Fig. 2(a). Accordingly, the slanted ZnO films have better crystalline quality than that of planar ZnO films. The intensities of (002) peak for both planar and slanted ZnO films show the overall trend of increase as annealing temperature increases, suggesting that better crystalline ZnO film can be obtained at higher annealing temperature which provides sufficient thermal energy for deposited atoms to diffuse, and thus redistributes them much orderly [18, 19]. In addition, as the annealing temperature increases, the full width at half maximum (FWHM) of ZnO (002) peaks decreases as well (plotted in Fig. 2(b)), indicating the average grain sizes along <002> ZnO films become larger. The grain sizes of ZnO films were calculated using Scherrer's equation and also plotted in Fig. 2(b). The grain size along <002> of slanted ZnO films grows slower (from 30 nm to 40 nm) than that of planar ZnO film (from 30 nm to 90 nm) at high annealing temperature. This probably is because, for the film deposited by OAD, the separation of nano-columns/rods is usually larger than that of film deposited by conventional means [20]. Hence, the increasing rate of grain size along <002> of slanted ZnO film is slower. Here has to note that the nano-columns/rods for planar and slanted ZnO films are parallel and inclined, respectively, to the surface normal direction (i.e. parallel to <002>); therefore, the derived grain size along <002> for slanted ZnO film cannot directly reflect the grain size along the axis of slanted columns/rods, which is different from that of planar ZnO films.

#229127 - $15.00 USD Received 8 Dec 2014; revised 7 Jan 2015; accepted 14 Jan 2015; published 21 Jan 2015

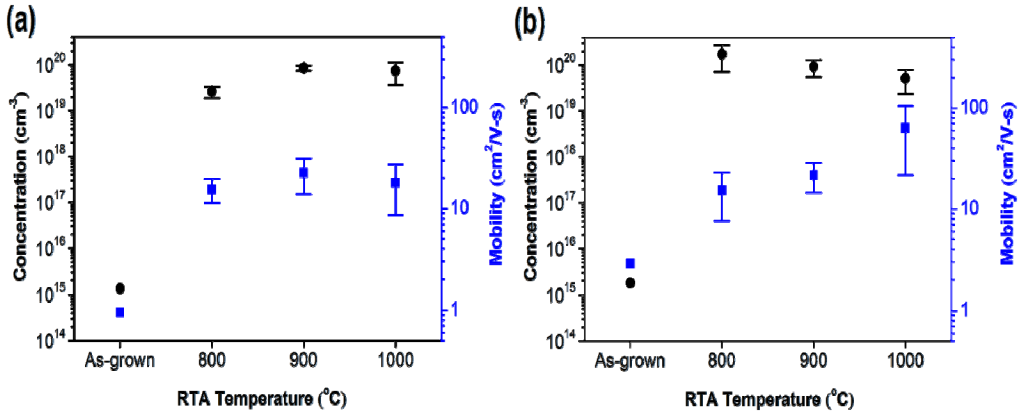

Fig. 3. The carrier concentration and mobility as function of RTA temperature for the (a) planar ZnO films and (b) slanted ZnO films. The carrier concentration and mobility of both as-grown samples are also plotted in the figure for comparison.

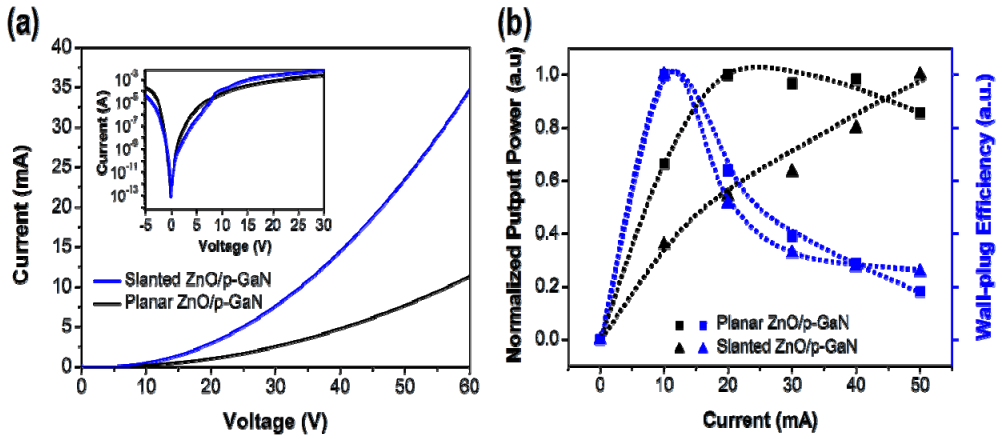

Fig. 4. (a) I-V curves of the slanted and planar ZnO/p-GaN LEDs. The inset shows the semi-log plot of the same I-V curves. (b) Normalized output power and wall-plug efficiency as function of injection current for planar and slanted ZnO/p-GaN LEDs. The dashed lines are guides to eye.

The electrical properties of ZnO films are also important for making LEDs. The Hall measurement shows both of the planar and slanted ZnO films with n-type conductivity. This agrees with the intrinsic n-type polarity of ZnO, and confirms that both of the planar and slanted ZnO films can be integrated with p-GaN to fabricate heterojunction LEDs. Figures 3(a) and 3(b) show the carrier concentration as function of annealing temperature (800–1000 °C) for the planar and slanted ZnO films, respectively. In general, the carrier concentrations of the planar and slanted ZnO films increase as annealing temperature increases and then reach a level between 10^{19}–10^{20} cm^{-3} at high annealing temperatures. The increase of carrier concentration is observed commonly in post-annealed ZnO films [21] and might relate to the formation energies of defects/impurities associated with the n-type carriers [22]. The mobility for the planar and slanted ZnO films are plotted in Figs. 3(a) and 3(b) as well, respectively. The mobility of planar ZnO film reaches to a value around 20 cm^2/V-s as annealing temperature higher than 800 °C. For the slanted ZnO film, the mobility increases as annealing temperature increases. The observation of mobility variation probably is due to the scattering of high carrier concentration (of order around 10^{20} cm^{-3}) [23]. Since the current will inject longitudinally and then spread laterally for the both planar and slanted n-ZnO/p-

#229127 - $15.00 USD Received 8 Dec 2014; revised 7 Jan 2015; accepted 14 Jan 2015; published 21 Jan 2015

GaN LEDs, the out-of-plane mobility is also important as in-plane mobility (extracted from Hall measurement). But since sapphire is an insulator, we are unable to extract the out-of-plane mobility for the samples of ZnO film on sapphire by using the methods we know (which are for materials grown on conducting substrates). Besides the (out-of-plane and in-plane) mobility, the carrier concentration as well as other factors, such as nano-sized effects, might also affect the performance of the planar and slanted n-ZnO/p-GaN LEDs. However, more investigations are needed in order to find out the dominant effect.

Based on the results of ZnO films on sapphire, the annealing conditions for ZnO films on p-GaN was set at 1000 °C for 1 min. Therefore, now we can discuss the ZnO/p-GaN heterostructures and devices. First, we investigate the electrical properties of the devices. Figure 4(a) shows the I-V curves of planar and slanted ZnO/p-GaN LEDs. The slanted ZnO/p-GaN LEDs have a turn-on voltage of 5 V, which is smaller than that of planar ZnO/p-GaN LEDs (10 V). Therefore, for same injection current, the slanted ZnO/p-GaN LEDs only need a smaller forward bias. Moreover, due to the inherent type-II band-alignment at the ZnO/GaN interface, the reverse currents of n-ZnO/p-GaN LEDs (shown in the inset of Fig. 2) could be greater than forward currents at the same absolute biases because of the carrier tunneling through the heterojunction [9]. Nevertheless, the slanted ZnO/p-GaN LED still exhibits a smaller leakage current (4.4×10^{-5} A) at −5 V than that of planar ZnO/p-GaN LED (1.9×10^{-4} A), suggesting it has better crystalline quality and less defect-related tunneling leakage than planar ZnO/p-GaN LEDs.

Figure 4(b) plots the normalized output powers for the slanted and planar ZnO/p-GaN as function of injection current. The output powers are normalized to the maximum output power we measured. Additionally, the wall-plug efficiency was calculated and also plotted in Fig. 4(b). The output power of planar ZnO/p-GaN LED saturates as injection current larger than ~20 mA. In consequence, its wall-plug efficiency reaches maximum as injection equal to 10 mA and then decreases as injection current increases. For slanted ZnO/p-GaN LED, on the other hand, the output power keeps increasing as injection current increases within the range we measured, although the increasing rate decreases at high injection current. Therefore, the wall-plug efficiency of slanted ZnO/p-GaN LED achieves its maximum value at injection current of 10 mA and then decreases but slower than that of planar ZnO/p-GaN LED as injection current increases. The possible reason for the change of output-power increasing rate and efficiency drooping at high injection current could be attributed to the device's overheating. This indicates that the slanted ZnO/p-GaN LEDs are better than planar ZnO/p-GaN LEDs for operating at high current. It shall be noted that although the junction area of the slanted ZnO/p-GaN LED is much smaller than that of the planar ZnO/p-GaN LED due to its porous geometry, the output powers of both devices are still comparable especially under high current operation.

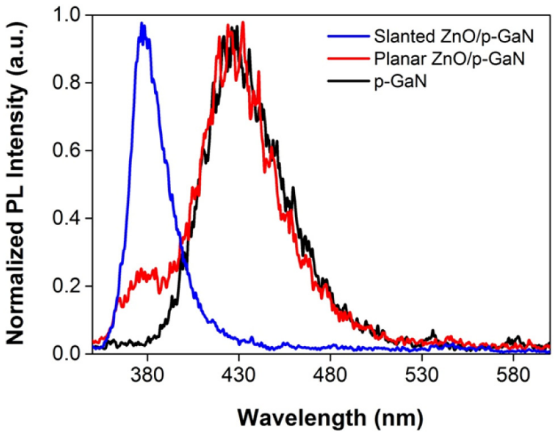

Fig. 5. Normalized PL spectra of planar and slanted ZnO /p-GaN heterostructures and p-GaN.

#229127 - $15.00 USD Received 8 Dec 2014; revised 7 Jan 2015; accepted 14 Jan 2015; published 21 Jan 2015

Next, we will examine the optical properties of fabricated LEDs. The normalized PL spectra of planar and slanted ZnO/p-GaN heterostructures are plotted in Fig. 5. The PL spectrum of p-GaN without ZnO film on top was also measured and is plotted for a comparison. The p-GaN shows an emission peak of wavelength around λ = 440 nm, which is commonly observed in p-GaN and typically attributed to the transition from conduction band or shallow donor to Mg acceptor levels in p-GaN. The PL spectrum of planar ZnO/p-GaN heterostructure also exhibits a dominant peak of wavelength around 440 nm with a small shoulder around λ = 380 nm. The emission peak of 440 nm is from the p-GaN since it has same peak position and similar line shape with p-GaN. The small peak around λ = 380 nm is attributed to the near-band-edge (NBE) transition of ZnO (shallow donor to valance band) [7, 24]. For the slanted ZnO/p-GaN heterostructures, a sharp and dominant peak with FWHM of 30 nm at λ = 380 nm is observed, which is also from the NBE transition of ZnO. In addition, different from the planar ZnO/p-GaN heterostructures, the PL signal from underneath p-GaN of the slanted ZnO films is not clearly seen. This is because the slanted ZnO film absorbs most of pumping light and results in weaker excitation to the p-GaN. This indicates that the slanted ZnO films on top of p-GaN have better quality than planar ZnO films on top of p-GaN. Moreover, the dominant emission peak around 380 nm of slanted ZnO/p-GaN heterostructures indicates that slanted ZnO/p-GaN heterstructures are more suitable for UV emission devices than planar ZnO/p-GaN heterostructures.

Finally, we will further investigate the electroluminescence of planar and slanted ZnO/p-GaN LEDs. The normalized EL spectra of planar and slanted ZnO/p-GaN LEDs for various injection currents are plotted in Figs. 6(a) and 6(b), respectively. The obtained EL spectra under different injection currents are then converted into 3D contour images as shown in Figs. 6(c) and 6(d) for planar and slanted ZnO/p-GaN LEDs, respectively. For planar ZnO/p-GaN LEDs, the EL spectra show only one broad emission peak of wavelength around 600 nm (2.07 eV) for injection current less than 20 mA. When injection current reaches 30 mA, another emission peak around λ = 400 nm (3.1 eV) starts to emerge out, and its intensity increases as injection current increases and becomes dominant as injection current larger than 40 mA. The peak of 630 nm probably relates to the transition of electron from ZnO conduction band to the deep defect level [25, 26]. The peak around 400 nm appeared at high injunction current should originate from the NBE transition of ZnO. For the slanted ZnO/p-GaN LEDs, the EL intensity become stronger as injection current increases, and show a dominant peak around 390 nm and a weak peak around 490 nm. Again, the 390 nm emission should be dominated by the NBE emission of slanted ZnO. The emission of 490 nm is probably related to the radiative interfacial recombination of the electrons from n-ZnO and holes from p-GaN [24], or to the energy transition from a shallow donor level to the V_{zn} level [22]. It should be noted that as the ODA creates slanted ZnO nanorods on the planar p-GaN layer, we should consider the hetero-junction structure with nano-sized geometry. The density of states (DOS) and the radiative recombination rate of injected carriers are hence quantized and enhanced while considering the quantum confinement effect. Consequently, most of injected electrons were confined within the slanted ZnO nanorods, and eventually recombined radiatively to emit ultraviolet light, even the electron concentration and mobility of the slanted ZnO film are both larger than those of p-GaN layer. Again, further studies are necessary to understand and confirm the recombination detail of injected carriers for such slanted ZnO/p-GaN hetero-junction LEDs. The peak position and FWHM of dominant peak for the planar and slanted ZnO/p-GaN LEDs are summarized in the inset of Fig. 6(b). The FWHM of planar ZnO/p-GaN LEDs emission depends on the emission colors. However, the FWHM of slanted ZnO/ p-GaN LEDs emission is narrow and retains around 15 nm. The dominant peak of the planar ZnO/p-GaN LEDs changes from 600 nm to 400 nm at high injection current. However, the slanted/p-GaN LEDs retain emission around 385-400 nm within the entire injection we applied. The small red shift of emission peak probably is due to overheating at large injection current. The photographs of planar and slanted ZnO/p-GaN LEDs under injection current of 30 mA are shown in the inset of Fig. 6(b) as well, which

#229127 - $15.00 USD Received 8 Dec 2014; revised 7 Jan 2015; accepted 14 Jan 2015; published 21 Jan 2015

emit reddish and bluish-white color, respectively. Accordingly, the slanted ZnO/p-GaN LEDs are more suitable for UV emission than the planar ZnO/p-GaN LEDs.

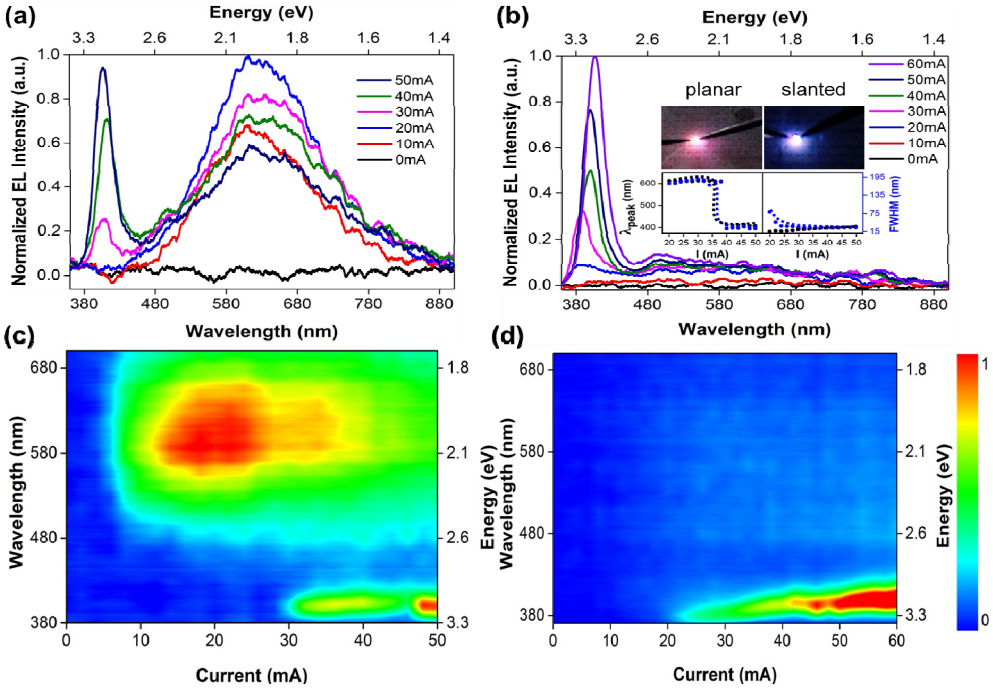

Fig. 6. The EL spectra of the (a) planar and (b) slanted ZnO/p-GaN LEDs under various injection currents. The position and FWHM of dominant peak versus injection current for the planar and slanted ZnO/p-GaN LEDs are shown in the inset of (b). The photographs of the planar and slanted ZnO/p-GaN LEDs under 30 mA are also shown in the inset of (b). (c) and (d) show the 3D contour images of EL spectra for the planar and slanted ZnO/p-GaN LEDs, respectively.

4. Conclusion

In conclusion, we compared the planar and slanted ZnO/p-GaN LEDs which are fabricated by conventional method and oblique angle deposition using RF sputtering system. Their electrical and optical properties were investigated systematically. Comparing with the planar ZnO/p-GaN LEDs, the slanted ZnO/p-GaN LEDs not only have smaller turn-on voltage but also retain bluish-white color luminescence within the injection current we applied. The results suggest that the slanted ZnO/p-GaN LEDs are more suitable for UV emission devices than the planar ZnO/p-GaN LEDs. This probably because the slanted ZnO films have better crystalline quality than planar one; however, a more detailed investigation, such as changing the slanted angles β and annealing temperatures and then investigating the evolution of these ZnO films, is needed in order to understand the mechanism and the dominant effect on the emission of the planar and slanted n-ZnO/p-GaN LEDs.

Acknowledgments

The authors gratefully acknowledge financial support from the National Science Council of the Republic of China (ROC) in Taiwan (contract nos. NSC 102–2218–E–009–017 and NSC 100–2112–M–003–006–MY3), and from the Ministry of Science and Technology in Taiwan (contract nos. MOST 103–2112–M–003–008–MY3 and MOST 104–2622–M–003–001–CC2). The authors would like to thank Mses. Su-Jen Ji and Chia-Ying Chien, and Prof. Chun-Hsien Chen of National Taiwan University for technical support in SEM experiments and fruitful discussions.